

Few-shot Learning for Domain-specific Fine-grained Image Classification

Xin Sun, *Member, IEEE*, Hongwei Xv, Junyu Dong, *Member, IEEE*, Qiong Li, Changrui Chen

Abstract—Learning to recognize novel visual categories from a few examples is a challenging task for machines in real-world applications. In contrast, humans have the ability to discriminate even similar objects with little supervision. This paper attempts to address the few-shot fine-grained recognition problem. We propose a feature fusion model to explore the largest discriminative features by focusing on key regions. The model utilizes focus-area location to discover the perceptually similar regions among objects. High-order integration is employed to capture the interaction information among intra-parts. We also design a Center Neighbor Loss to form robust embedding space distribution for generating discriminative features. Furthermore, we build a typical fine-grained and few-shot learning dataset *miniPPPlankton* from the real-world application in the area of marine ecological environment. Extensive experiments are carried out to validate the performance of our model. First the model is evaluated with two challenging experiments based on the *miniDogsNet* and Caltech-UCSD public datasets. The results demonstrate that our model achieves competitive performance compared with state-of-the-art models. Then, we implement our model for the real-world phytoplankton recognition task. The experimental results show the superiority of the proposed model compared with others on the *miniPPPlankton* dataset.

Index Terms—gansha1 Computer vision; Few-shot learning; Representation learning

I. INTRODUCTION

RCENT years we have witnessed significant progress in computer vision [1], [2]. Thanks to large-scale of labeled training data, e.g., ImageNet [3], deep convolutional neural networks (ConvNets) are able to successfully learn robust feature representations and achieve excellent performance in recognition tasks [4], [5], [6]. Although it has high accuracy in various labeled datasets, the generalization ability of the ConvNet model is still weak. In particular, the ConvNet model is difficult to quickly identify a novel category using only one or a few labeled samples (i.e., those samples do not exist in the initial training process, usually called support set).

However, humans are able to recognize new objects easily with very little supervision [7]. For example, kids have no problem to generalize the concept of “panda” from only one picture. Furthermore, experts will be faster to understand novel concepts with prior professional knowledge. This work focuses on the task that recognizing novel visual categories after seeing just a few labeled examples. Research on this subject is often termed *few-shot learning*. The essence is that the human few-shot generalization ability only occurs when new categories can be understood in the context of prior knowledge [8].

X. Sun, H. Xv, J. Dong, Q. Li, C. Chen are with the Department of Computer Science and Technology, Ocean University of China, Qingdao, P.R.China e-mail: sunxin@ouc.edu.cn.

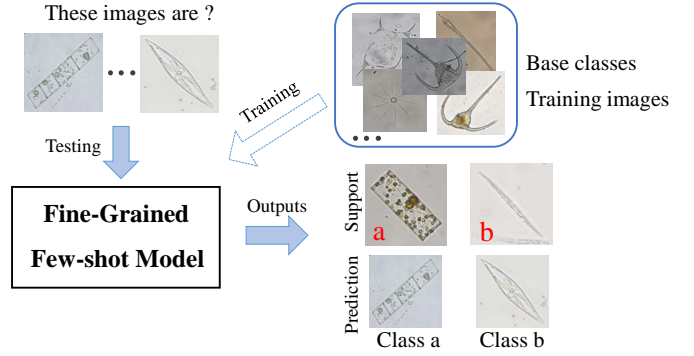


Fig. 1: A brief illustration of fine-grained few-shot recognition. The ‘support’ represents labeled samples, and query images will get predicted results based on the similarity with the support samples.

In contrast to the common image classification problem in daily life (e.g., ImageNet), most of the real-world scenarios face few-shot problems, particularly the fine-grained few-shot recognition problem. For example, marine biologist pays great attention to the phytoplankton recognition problem which is a typical fine-grained and few-shot learning issue. Phytoplankton is an essential part of the marine food chain and plays an important role in the global carbon cycle, energy flow and information transfer of aquatic ecosystems [9], [10]. The change of their abundance, e.g. eutrophication or pollution, is a significant indicator of the oceanic ecosystem’s health [11]. It is therefore very important to automatically identify phytoplankton in a certain area of the ocean [12]. However, collection of phytoplankton image samples is very difficult. It is commonly accomplished by professional instruments such as electron microscope. Only a few samples of valuable categories can be discovered in one expensive sampling task. This poses a great challenge for the machine learning task to train a classifier with a large number of classes and only a few examples. Therefore, the fine-grained and few-shot model is critical for domain-specific issues and has become one of the important topics in the computer vision area.

Most of the few-shot learning methods fall under the umbrella of metric-learning [13], [14], [15], [16]. Since labeled samples of novel categories are severely limited, the typical dot-product based classifier (e.g., Last linear layer of a ConvNet model) faces serious over-fitting and class-imbalance problems after fine-tuning the support set. The metric-learning approaches try to solve these problems by placing new classes

in a metric space (e.g., Euclidean or cosine distances) that can easily separate classes. For instance, Matching Networks [13] can be interpreted as a nearest-neighbor classifier which can be trained end-to-end over the cosine distance. Notably, the training procedure has to be chosen carefully so as to match inference at the test stage. Each episode is designed to mimic the few-shot tasks by subsampling classes as well as data points (e.g., every episode sampling 5 classes and each class has 5 labeled samples). Prototypical Networks [14] handles the few-shot tasks by calculating the Euclidean distance between the embedding points of query set and prototype representation of support set. Meanwhile, the pre-defined metric is no longer used in Relation Networks [16]. It uses concatenated feature maps from the query and support images to distinguish similar and dissimilar.

The important aspects of such models are the relation among feature representations of novel classes and the placement of a query image within the metric space. Thus, the key to success in few-shot metric tasks is twofold. One is robust features from a well-trained feature extractor. The other is an effective classifier including good metrics. However, the above-mentioned methods are not conducive to ConvNets for extracting robust features and will also sacrifice the accuracy of initial categories [17]. Most of the few-shot methods pay much attention to learning a deep distance metric to compare query images with the labeled images, while ignoring the importance of mining the discriminative features from the few labeled samples. Motivated by the above observation, our work focuses on exploring discriminative representations, especially for the domain-specific few-shot tasks (i.e., fine-grained few-shot classification). The overview of our tasks is shown in Fig. 1. We propose a Feature Fusion Model for obtaining more discriminative information from focus areas, and we also design a loss function (Center Neighbor Loss) to help the whole architecture to learn better feature space distributions.

For the special fine-grained few-shot visual problem, we further build a microimage dataset of phytoplankton, i.e., **miniPPlankton**. Unlike toy datasets for few-shot learning in literature¹, the **miniPPlankton** dataset comes from the real-world tasks and can be used to evaluate fine-grained and few-shot methods. It illustrates a typical fine-grained and few-shot problem in marine biological science.

The main contributions of this paper are as follows:

- We propose a feature fusion model to explore the features by focusing on the key regions. It utilizes focus-area locations to discover the perceptual similarity regions between objects. Meanwhile, high-order integration is used to capture the interaction information of intra-parts.
- We design a Center Neighbor Loss function to form robust feature space distributions for generating discriminative features, to accomplish the fine-grained few-shot visual categorization task.
- We carry out fine-grained few-shot classification experiments on *miniDogsNet* [15] and *Caltech-UCSD Birds* [18] datasets, and achieve competitive performance with state-of-the-art methods.

- We build a domain-specific fine-grained and few-shot dataset **miniPPlankton** for the real-world phytoplankton recognition problem. Experiments on the **miniPPlankton** show the superiority of the proposed model compared with other models.

The rest of this paper is organized as follows. Section II summarizes the related works. Section III formally describes our model. Section IV presents the experimental results. Finally, we conclude in Section V.

II. RELATED WORK

Deep convolutional neural networks have made significant achievements for a wide range of visual tasks [19], [20]. Nevertheless, for fine-grained image categorization [21], it remains quite challenging to obtain the discriminative representations. In particular, it is a novel challenge to classify fine-grained images using only a few labeled sample images. The convolutional neural networks usually require thousands of labeled examples of each class to saturate performance. However, it is impractical to collect large amounts of annotated data, especially the domain-specific dataset that requires expert knowledge. Recently, there is a resurgence of interest on few-shot learning. In the following, we briefly discuss the most relevant approaches to our work.

A. Metric learning

Metric learning is a long-standing problem in computer vision. It has been successfully applied to face recognition [22], [23] and fine-grained image classification [24], [25]. The core idea is to learn an embedding function that the samples of the same category are closer than those of different classes. Once the embedding function is learned, the query images will be classified.

Siamese network [26] consists of two identical sub-ConvNets that minimize the distances between paired data with the same labels while keeping the distances with different labels far apart. It gains much of attention due to its superior performance in face recognition [22], [23]. However, the contrastive embedding requires that the training data has precise pair-wise distances, which is difficult to satisfy in practice. Triplet loss [27] attempts to focus on relative distances rather than absolute pair-wise distances. Each triplet contains three images from two different classes that constituted positive pairs and negative pairs. Triplet loss also has been used to automatically learn feature representations that same classes are closer than those of different categories. It has been widely implemented in face recognition [28] and fine-grained tasks [25]. However, the problem of triplet loss is dramatic data expansion when we select triplets. The FaceNet [29] proposes an online strategy by selecting semi-hard negative examples to avoid dramatic data expansion and local extremum. Furthermore, center loss [30] can obtain highly discriminative features for robust face recognition. And it is unnecessary to design the sampling strategy carefully as contrastive loss and triplet loss do. The center loss has shown benefits in face identification. However, its performance is unknown for the fine-grained few-shot tasks. We will first carry out experiments to illustrate its

¹Existing datasets are usually resampled from large-scale datasets.

advantages and disadvantages. Then we further design a Center Neighbor Loss for achieving a robust embedding space.

B. Attention mechanism

Recent years, attention mechanisms have been widely used in machine translation [31], image generation [32], and weakly-supervised tasks [33], [34]. For CNNs, it is really important to know which part of the images worth paying attention to. The self-attention [35] method calculates the correlation matrix between each spatial point in the feature map; then the attention guides contextual information aggregation. It is differentiable and can be trained using backpropagation. Attention mechanisms also involve some works based on visualization of CNNs, which visualize CNN predictions by highlighting ‘important’ pixel (i.e., the attention area of one image). The idea is widely used in weakly supervised object localization (WSOL) [36], [33]. WSOL refers to learn objects locations only using image-level labels. The objects’ locations are related to the focus area of images. Class Activation Mapping (CAM) [36] modifies classification networks by replacing fully-connected layers with convolutional layers, and global average pooling [37] aggregates the features of the last convolutional layer to locate object. Grad-CAM [33], a generalization of CAM, is applicable to a significantly broader range of ConvNets without modifying models anymore. The above methods show deep learning networks already have some kind of a built-in attention mechanism. It is normally used for initial object seeds in weakly-supervised semantic segmentation [38]. The attention mechanism is a possible way for learning robust representation. In this work, we introduce the focus-area location mechanism Grad-CAM to find regions with discriminative features.

C. Feature fusion in CNNs

A large amount of approaches attempt to use multiple layers’ features to improve the performance in computer vision tasks [39], [40], [41]. U-Net [39] associates low-level and high-level features to fully use the synthetic information. FPN [40] introduces a top-down structure to combine the different level features together to enhance the performance. DenseNet [6] uses dense skip-connections to encourage feature reusing. And Cai et al. [41] use high-order integration of hierarchical convolutional activations for fine-grained classification, which improved the performance greatly. Compared with the fully connected layers for capturing global semantic information, the convolution layers preserve more instance-level details and exhibit different discriminative capacities, which are more meaningful to the fine-grained few-shot tasks.

To acquire a better feature representation, we propose a feature fusion model contains two components. One is the integration of high-order representations with deep ConvNets, and the other is the focus-area location mechanism for finding discriminative regions.

D. Plankton Image Classification

Marine phytoplankton is the foundation of the marine ecosystem [42]. It is an ecological concept that refers to tiny

plants that float in the water. As the most important primary producer in the ocean and the global ecological environment, phytoplankton activates the marine food chain. In addition, phytoplankton also participates in the biogeochemical cycle of biogenic elements such as carbon, nitrogen, and phosphorus. Therefore, as people pay more attention to global environmental changes, plankton image classification² is becoming critically important in the ocean ecosystems research.

The research into phytoplankton community structure mainly relies on scientific research personnel to manually identify and count through the microscope, most of which belong to the non-in situ observation method. These methods are usually time-consuming, labor-intensive and needs strong professional knowledge. To solve these problems, in traditional machine learning, the bagging-based architecture [43] and SVM [44] are applied to plankton classification effectively. In recent years, Orenstein et al. [45] publicly released a large-scale database WHOI-Plankton for plankton classification. Under the 3 million labeled images of WHOI-P, the existing ConvNet architecture can be directly applied to the plankton classification [12]. Then, to overcome the class-imbalance problem of WHOI-P, Lee et al. [11] incorporate transfer learning by pre-trained CNN with class-normalized data and fine-tuning with original data. Interestingly, concurrently to us, Schroder et al. [46] also notice the importance of classifying plankton only using a few labeled samples. They directly use weight Imprinting [47] to enable a neural network to recognize small classes immediately without re-training. In this work, we not only build a few-shot phytoplankton dataset but also design a universal model to accomplish the few-shot task of natural images and phytoplankton images.

III. METHODOLOGY

A. Notation

For few-shot classification, there is a base train dataset $\mathcal{D}_{base} = \{(x_i, y_i)\}_{i=1}^N$ consisting of N labeled images, where y_i is the label of image x_i . Crucially, the model must distinguish a set of novel categories $\mathcal{Q} = \{(x_j, y_j)\}_{j=1}^{N_q}$ with a few training examples per category. These training examples are called support set, i.e., $\mathcal{S} = \{(x_i^s, y_i^s)\}_{i=1}^{N_s}$ ($N_s = K * C$) which contains K labeled examples for each of C unique novel classes. \mathcal{Q} acts as the unlabeled query set. Here $\mathcal{S} \cup \mathcal{Q} = \mathcal{D}_{novel}$ and $\mathcal{D}_{base} \cap \mathcal{D}_{novel} = \emptyset$. This target few-shot task is named C -way K -shot.

B. Model

An overview of our method is illustrated in Fig. 2, which mainly consists of three parts. Firstly, we implement a *ConvNet-based feature extractor* to extract primary features of input images. Then, a *feature fusion model* is designed to locate focus regions and generate feature representation, which is critical in our tasks. Finally, a classifier distinguishes query images of the set \mathcal{Q} .

²We no longer distinguish the image classification of phytoplankton and zooplankton separately.

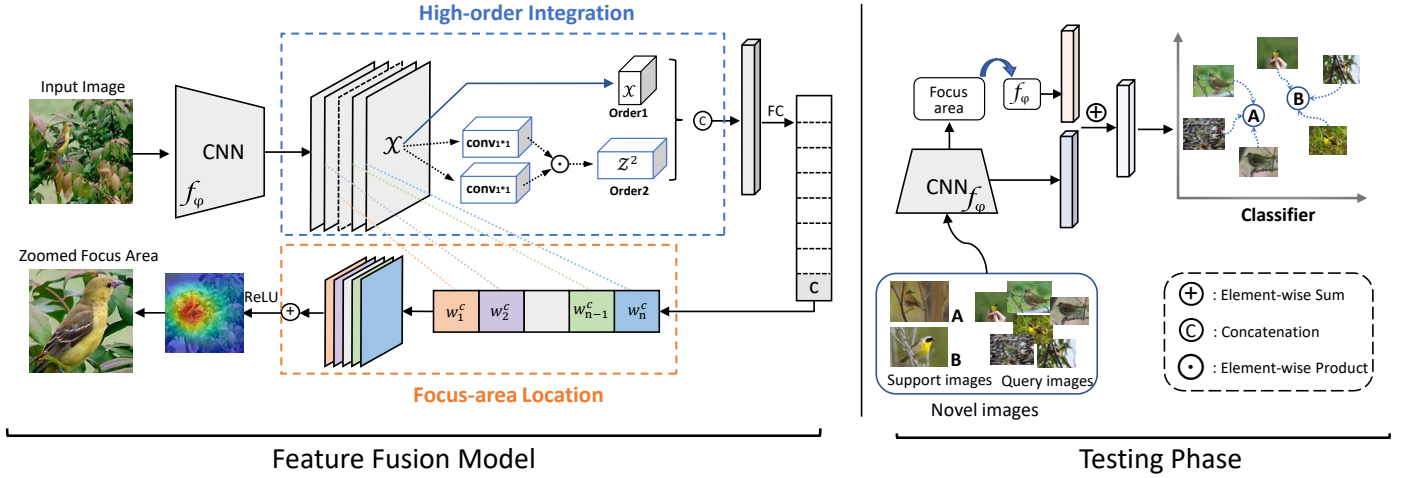


Fig. 2: The overview framework of our method. It consists of a *ConvNet-based feature extractor* f_ϕ , a *feature fusion model* which is formed by focus-area location mechanism and high-order integration, and a *cosine-similarity based classifier*. During the testing process, we classify unlabeled samples by comparing the cosine similarities of support set \mathcal{S} and query set \mathcal{Q} .

1) *ConvNet-based feature extractor*: A feature extractor f_ϕ , parameterized by a ConvNet (e.g., ResNet [5]), maps an input image $x \in \mathbb{R}^N$ to a d -dimensional feature vector $f_\phi(x) \in \mathbb{R}^d$. As a classification model, f_ϕ has a dot-product based classifier $C(\cdot|W)$ (e.g., Last linear layer), where $W = \{w_i \in \mathbb{R}^d\}_{i=1}^K$ is the set of K base classes weight vectors. We can get the probability scores of the base training categories by calculating $C(f_\phi(x)|W)$ and optimize the feature extractor by back-propagation.

2) *Feature fusion module*: For few-shot learning, it is pivotal to mine the largest support information from the support set \mathcal{S} . We propose a feature fusion model which utilizes the focus-area location and high-order integration to generate feature representation for the few-shot tasks. As shown in Fig. 2, it consists of two components: (1) high-order integration, and (2) focus-area location.

High-order integration. The recent progress of fine-grained classification demonstrates that the high-order representations with ConvNets can greatly improve its performance [41], [48]. Intuitively, the key for fine-grained few-shot tasks is to discover and represent the regions within the same category that have a closer appearance and exhibit discriminative areas between the different categories.

We assume that $\mathcal{X} \in \mathbb{R}^{K \times M \times N}$ is a 3D feature map from the convolutional layers, where $x \in \mathcal{X}$ is a K -dimensional descriptor of one particular location region $p \in M \times N$. The linear predictor \mathcal{W} on the high-order statistics of \mathcal{X} could be formulated as follow.

$$f(\mathcal{X}) = \langle \mathcal{W}, \sum_{x \in \mathcal{X}} \phi(x) \rangle \quad (1)$$

where $\sum_{x \in \mathcal{X}} \phi(x)$ denotes the high-order statistics characterized by a homogenous polynomial kernel [49]. The \mathcal{W} can be approximated by rank-one decomposition. The tensor rank decomposition expresses a tensor as a minimum-length linear combination of rank-1 tensors. The outer product of vectors

$\mathbf{u}_1 \in \mathbb{R}^{K_1}, \dots, \mathbf{u}_r \in \mathbb{R}^{K_r}$ is the $K_1 \times \dots \times K_r$ rank-1 tensor that satisfies $(\mathbf{u}_1 \otimes \dots \otimes \mathbf{u}_r)_{k_1 \dots k_r} = (\mathbf{u}_1)_{k_1} \dots (\mathbf{u}_r)_{k_r}$. The \mathcal{W} can be rewritten as, $\mathcal{W} = \sum_{d=1}^D a^d \mathbf{u}_1^d \otimes \dots \otimes \mathbf{u}_r^d$, where a^d is the weight for d -th rank-one tensor, D is the rank of the tensor if D is minimal. Thus, Eq.1 can be reformulated as,

$$f(\mathcal{X}) = \sum_{x \in \mathcal{X}} \left\{ \langle \mathbf{w}^1, \mathbf{x} \rangle + \sum_{r=2}^R \sum_{d=1}^D a^{r,d} \prod_{s=1}^r \langle \mathbf{u}_s^{r,d}, \mathbf{x} \rangle \right\}, \quad (2)$$

$$= \langle \mathbf{w}^1, \mathbf{x} \rangle + \sum_{r=2}^R \langle \mathbf{a}^r, \mathbf{z}^r \rangle$$

where the $\mathbf{z}^r = \prod_{s=1}^r \langle \mathbf{u}_s^{r,d}, \mathbf{x} \rangle \in \mathbb{R}^{D_r}$ characterizes the degree- r variable interactions under a single rank-1 tensors. The \mathbf{z}^r can be calculated by performing r -th 1×1 convolutions with D^r channel [50], i.e., $\mathcal{Z}^r = \{\mathbf{z}^r\} = \prod_{i=1}^r \text{conv}_{1 \times 1 \times D^r}^i(\mathcal{X})$. In our feature fusion operation, as shown in Fig. 2, we integrate 2-order representations to capture more complex and high-order relationships among parts. After that, we perform global average pooling (GAP) [37] to further aggregate features.

Focus-area location. Existing studies show that learning from object regions could benefit object recognition at image-level [51], [52]. Such focus-area in an image which benefit few-shot learning. During the training procedure, f_ϕ can generate focus-areas of images by Grad-CAM [33], as formulated below.

$$L_{\text{Grad-CAM}}^c = \text{ReLU} \left(\sum_k \alpha_k^c A^k \right) \quad (3)$$

where α_k^c denotes the weight of the k -th feature map for category c . α_k^c can be calculated by the following formula:

$$\alpha_k^c = \frac{1}{Z} \sum_i \sum_j \frac{\partial y^c}{\partial A_{ij}^k} \quad (4)$$

where Z is the number of pixels in feature map, y^c is the classification score corresponding to the category c , A_{ij}^k denotes the pixel value at the location of (i, j) of the k -th feature map.

Grad-CAM has the ability to locate the focus areas that belong to the corresponding category. In this work, we utilize Grad-CAM to generate base categories' focus regions $\mathcal{H}_{base} = \{(x_i^h, y_i^h)\}_{i=1}^N$. However, the ConvNet extractor can not give a correct response of c in Eq.4, when a novel category appears. To our delight, we find that the model have accumulated lots of meta-knowledge in the domain field (e.g., Ornithology) during the training process of $\mathcal{D}_{base} = \{(x_i, y_i)\}_{i=1}^N$. The concepts of novel categories can be made up of various meta-knowledge, which are already embedded in neural networks. For example, if someone has never seen the tiger, she/he might think it has many close parallels to a cat (learned before). The reason is that the attention locations of human on the new category tiger and known category cat are similar to each other. For fine-grained few-shot tasks, although we don't know the ground truth of the novel samples, the unseen class always has similar regions to the \mathcal{D}_{base} , such as bird's mouths and wings. And the base classifier will classify the new sample into the most similar class in \mathcal{D}_{base} . Therefore, it is still possible to use Grad-CAM generating good focus-area location \mathcal{H}_{novel} on the unseen categories for enhancing feature representation.

Telling the neural network the regions of rich discriminative information will form a more robust representation. This step is similar to the data augmentation of input space. However we only mine the available information on input itself without using the extra data augmentation.

3) *Classifiers*: Generally, the ConvNet's classifier uses the dot-product operator to compute classification scores: $s = z^T * w_k^b$, where z is the feature vector extracted by ConvNets and w_k^b is the k -th classification weight vector in W_{base} . It is trained from scratch by thousands of optimization steps (e.g., SGD). In contrast, the W_{base} is not adapted to the new categories and it is difficult to find the proper classification weights W_{novel} with only a few samples and optimization steps. To address this critical problem, a classifier should be implemented to distinguish the new categories. To the best of our knowledge, current researches commonly choose one of the following classifiers to gain their best performance, such as SVM [53], cosine-similarity [47] and nearest neighbor.

SVM. SVM classifier has achieved an excellent performance for small training data in few-shot learning [53]. Essentially, unlike deep learning methods which need large-scale training data to learn generalization ability within classes, SVM is a classical transductive inference method aiming to build a model that is applicable to the problem domain.

Nearest neighbor. The Euclidean-based nearest neighbor method uses feature vector z_s to build a prototype representation of each novel class for the few-shot learning scenario. Then it classifies the unlabeled data by calculating the distance from each query embedding point to the prototype.

Cosine classifier. The cosine classifier has been well established as an effective similarity function for few-shot tasks [13], which classifies samples by comparing the cosine similarity between z_s and z_q .

$$similarity = \frac{z_s \cdot z_q}{\|z_s\| \|z_q\|} = \frac{\sum_{i=1}^n (z_s^i * z_q^i)}{\sqrt{\sum_{i=1}^n (z_s^i)^2} * \sqrt{\sum_{i=1}^n (z_q^i)^2}} \quad (5)$$

where z_s and z_q denote the support and query feature vector with n -dimensions generated from the above-mentioned Feature Fusion Model, respectively. Here, after testing the performance of three classifiers, we will choose the best one.

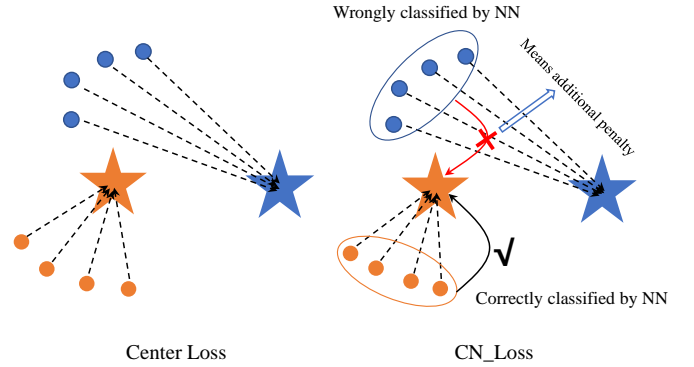


Fig. 3: The center loss is simply pulling the samples into the class-center (entagram). While CN_loss adds additional penalties to the sample of the wrong classification (red fork symbol) using nearest-neighbor.

C. Objective function

The loss function is important to let the neural network generate separable representations for the unseen classes. Some kinds of loss functions in the area of face recognition are useful for few-shot tasks. For example, Siamese Nets [54] applies contractive loss to few-shot tasks, so that neural networks can learn to distinguish similarities from dissimilarities. For fine-grained few-shot tasks, it is critical to develop an effective similarity constraint function to improve the discriminative power of the feature representations. Center loss [30], which was first proposed for the face recognition problem, simultaneously learns a center for deep features of each class and penalizes the distances between the deep features and their corresponding class centers. Suppose there are K classes for samples, k^i is the category of the image x_i and $z_i = f_\varphi(x_i)$ denotes the deep features extracted from x_i . Here is the formulation for center loss:

$$\mathcal{L}_c = \frac{1}{2} \sum_i^n \|z_i - c_{k^i}\|_2^2. \quad (6)$$

The $c_k \in \mathbb{R}^K$ denotes the k -th class center of deep features. The formulation effectively characterizes the intra-class variations.

However, all training samples are treated equally when a center loss function minimizes the intra-class variations, regardless of whether the sample is easy or hard to pull into the center point. We observe that it is difficult to quickly form a

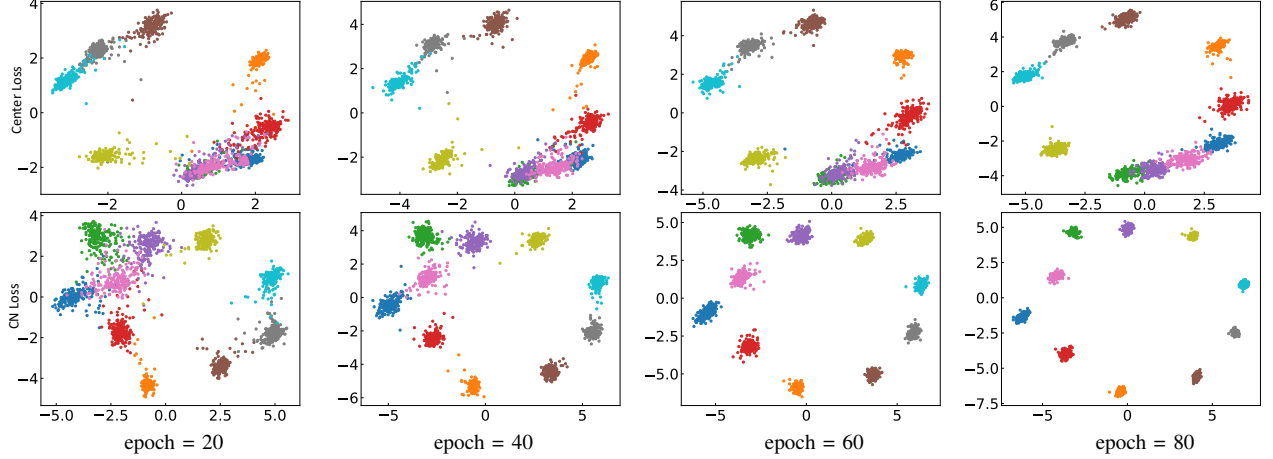


Fig. 4: The distribution of deeply learned features under Center loss and CN_loss. Different colors denote different classes.

good embedding space distribution even for a simple dataset such as Fashion-MNIST [8]. Intuitively, for the fine-grained tasks, the difference among classes is extremely small. It is not enough to form a good distribution by simply pulling the feature vector into the class center. It is critical to impose special penalties on the samples which are difficult to approach the center during the training process. To this end, we further propose the Center Neighbor Loss (CN_Loss) function \mathcal{L}_s to form robust embedding space distribution as following.

$$\mathcal{L}_s = \mathcal{L}_c + \beta \cdot \mathcal{L}_N \quad (7)$$

β is the balance parameter for penalty term \mathcal{L}_N . \mathcal{L}_N is a negative log-probability for samples that are not classified to the correct class center. The \mathcal{L}_N can be formulated as following.

$$\mathcal{L}_N = -\log \frac{\exp(-E(\bar{z}^k, \mathbf{c}_k))}{\sum_{k' \in K} \exp(-E(\bar{z}^{k'}, \mathbf{c}_{k'}))} \quad (8)$$

$\bar{z}^k = \text{Avg}(\sum_{x_i^k \in \mathcal{D}_{base}} f_\varphi(x_i^k))$ is the k -th class average feature vector contained in every batch, and $E(\cdot, \cdot)$ denotes the *Euclidean* distance.

The schematic is shown in Fig. 3. We take the center points learned from the last iteration as support points and use Euclidean-based nearest neighbors to classify the current batch of samples. With the penalty \mathcal{L}_N , each cluster will gather faster and perform robustly.

Ideally, the class center c_k should be updated as feature vectors changed. That means we should take the entire training set into account and average the deep features of each class in each iteration, which is not feasible in practice. To solve this problem, we implement the solution suggested for center loss [30]. First of all, we perform the update procedure based on mini-batch. The centers are computed by averaging the features of every category in each iteration. Secondly, we use the centers learned from the last iteration to classify the current batch samples by Nearest Neighbor Algorithm and punish the mislabeled samples. At last, we fix the learning rate of the centers as 0.5 to avoid large perturbations caused by mislabeled samples [30].

IV. EXPERIMENTS

A. Experimental design

For rare categories, it's extremely difficult to collect sufficient and diverse training images. Currently, most of the previous few-shot learning methods take the *miniImageNet* dataset [13] to test their performance with 5-way 1-shot or 5-way 5-shot assumptions. However, the *miniImageNet* consists of 60,000 color images with 100 classes of which 64 classes for training. The training data is enough to learn a good feature extractor for a common few-shot classification task, and nearly 80% accuracy has been already achieved recently [53]. In this paper, we focus on the fine-grained few-shot classification tasks. To this end, we design three different experiments on Caltech-UCSD Birds [18] datasets, *miniDogsNet* [15] and *miniPPlankton*.

For the *miniDogsNet* dataset [15], we only use **10 classes** for training, and conduct 5-way experiments with both 1-shot and 5-shot settings. We will compare our method with other well known techniques including Matching Networks [13], Prototypical Networks [14], Relation Networks [16], MAML [55] and GNN [56] for the 5-way experiments with 1-shot and 5-shot. All methods are also training on these 10 classes. In order to ensure the fairness of comparison, we unify the MatchingNets, PrototypicalNets and Imprint' feature extractor to ResNet. Considering the Relation Networks and MAML using meta-learning training strategy is difficult to train using deep ConvNets, we do not to struggle to adjust their network architecture anymore.

In real-world scenarios, humans face a large number of novel categories to be recognized. 5-way experiments only for toy examples in papers. Currently, one state-of-the-art research work [47] implemented the Caltech-UCSD Birds dataset [18] for 100-way few-shot learning problem, which is much practical. Here we will carry out experiments on the Caltech-UCSD Birds dataset with the same setting of Imprint [47]. That means we investigate the accuracies on all the novel classes. As the above-mentioned methods including RelationNets [16] are designed for only 5-way experiments, it

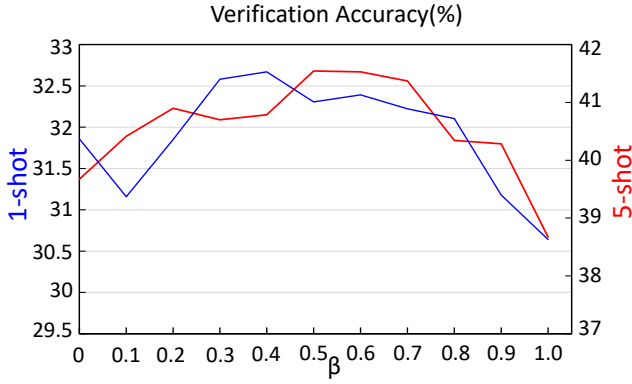


Fig. 5: The verification accuracies with different β .

is difficult to accomplish the 100-way procedure. For example, RelationNets [16] requires huge GPU memory spaces for the 100-way training. Therefore, we only set the recent work Imprinted Weights [47] as the comparison. For few-shot tasks, the Imprinted Weights [47] described how to add a similar capability to ConvNet classifier by directly setting the weights of the final layer from novel labeled samples. Essentially, the core of Imprinted Weights method is cosine similar function. Therefore, in the following experiments, **the baseline (ResNet + cosine classifier) we use is the same as the Imprint in nature.**

In real-world scenario application, for *miniPPlankton*, we will compare our method with MatchingNets, PrototypicalNets, Imprint. All of above the methods are re-implemented with ResNet as the backbone feature extractor.

B. Implementation details

ResNet18 [5] is employed as the feature extractor f_φ . Same as Wen [30], our feature extractor needs to train under the joint supervision of softmax loss and CN_loss. During training, we initialize the learning rate of the softmax loss as 0.001 and half it every 20 epochs and we only use the last feature map as the input of high-order integration. During testing phase, for *miniDogsNet* and Caltech-UCSD Birds, raw support image and zoomed focus-area are uniformly resizing into 224×224 and send them to f_φ to form robust feature vector. For *miniPPlankton*, due to the specificity of the phytoplankton image, e.g., target is scattered shape. Therefore, slightly differing from the structure Fig. 2, we do not use the backbone network to extract the focus-areas' feature. Here we resize focus-area into 84×84 to train a shallow CNN (four convolution blocks). Through the shallow CNN, the testing focus-area's feature will also be merged with the original image's feature.

C. Configuration variants

CN_Loss. We conduct experiments to visualize the performance of Center loss and CN_loss on Fashion-MNIST [8]. It consists of 60,000 training examples and 10,000 for testing. Each example is a 28×28 gray-scale image, associated with a label from 10 classes. We generate deep features individually

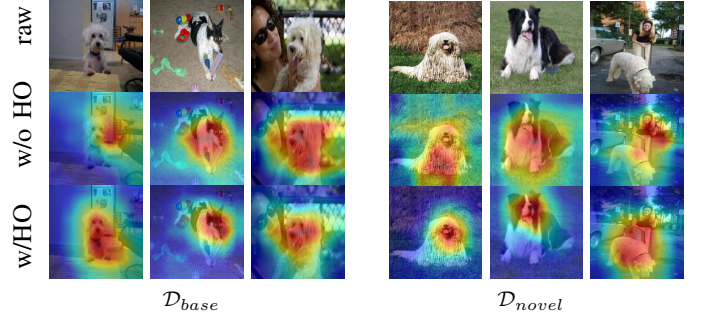


Fig. 6: Visualization results with Higher-order Integration and without it. The left three columns show the focus regions on the \mathcal{D}_{base} , while the right three denote focus regions of novel samples from \mathcal{D}_{novel} .

with CN_Loss and Center loss under the joint supervision of softmax loss. Datasets such as MNIST or Fashion-MNIST can more intuitively reflect the difference of feature space distribution brought by different loss functions [57]. A more robust feature space distribution usually means we have a better feature extractor. The space distribution results are shown in Fig. 4. We can see that, CN_loss can quickly form the cluster of each class. The hyperparameter β in Eq. (7) is the balance for penalty term \mathcal{L}_N . We investigate the performance of our model with different hyperparameter β on *miniDogsNet*'s validation set. As shown in Fig. 5, it is very clear that the center loss (i.e., $\beta = 0$) is not a good choice for few-shot classification problem. The best performance can be achieved in the case of $\beta \in [0.4, 0.6]$.

High-order integration. The high-order integration could help us to capture more complex and high-order relationships among different intra-parts to get better attention maps. As shown in Fig. 6, it helps to focus on the discriminative regions of the image.

Focus-area location. We investigate the role of Focus-area Location on our fine-grained tasks. Section III-B3 briefly described cosine classifier used in our tasks. We will also illustrate the performance of different classifiers on the fine-grained few-shot classification. Table 7 shows the accuracies on different tasks with the same feature extractor setting. For the *miniDogsNet* dataset, the cosine classifier could achieve the highest accuracy on the validation set. And focus-area location achieves positive improvement. For the CUB-200-2011 dataset, both cosine classifier and SVM can achieve nice performance. Especially, we also find that the focus-area location greatly improves the accuracies of SVM classifier.

D. Caltech-UCSD Birds

The Caltech-UCSD Birds dataset [18] includes 200 fine-grained categories of birds with 11,788 images. The sample images are shown in Fig. 8, the dataset is also marked with attribute information for each class. We take pre-trained ResNet18 [5] with ImageNet as the feature extractor f_φ . Train/test split setting is followed the suggestion of Imprinted Weights [47]. Here, 100 novel classes are required to be

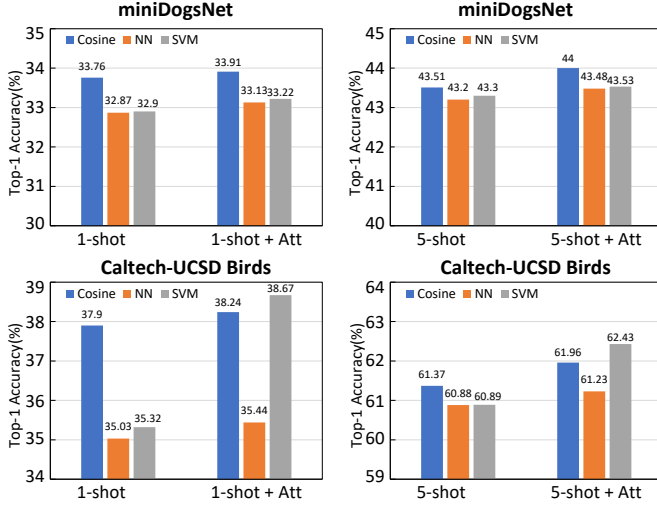


Fig. 7: The accuracy of three classifiers with and without Focus-area Location under 1 shot and 5 shot assumptions. 'Att' means Focus-area Location.



Fig. 8: Random samples from two classes of the Caltech-UCSD Birds dataset.

distinguished, which is very challenging and similar to the real-world scenario. The cosine classifier is employed to recognize the novel categories.

As shown in Table I, for all novel categories classification, we observe that the high-order module and CN_Loss function are beneficial to our tasks. In particular, the information of focus-areas brings considerable improvement in accuracy on the 5-shot setting. It is also important to illustrate the capability of recognition performance on the all categories. Because most of the few-shot classification methods sacrifice the recognition accuracy on the base categories that the ConvNet was trained on [17], we evaluate the performance on dataset of $\mathcal{D}_{base} \cup \mathcal{D}_{novel}$ [47]. Table I and table II show that our model achieves promising accuracies on the novel categories while at the same time it does not sacrifice the recognition performance of the base categories \mathcal{D}_{base} .

N -shot	1	2	5
Imprint (ori)[47]	21.26%	28.69%	39.52%
Imprint + Aug (ori)	21.40%	30.03%	39.35%
Imprint (re)	28.77%	39.25%	49.33%
ResNet + H	30.14%	38.46%	49.83%
ResNet + CNloss	29.86%	39.45%	50.68%
ResNet + CNloss + H	30.17%	40.10%	50.78%
ResNet+CNloss+H+Att	30.82%	40.85%	51.95%

TABLE I: Top-1 accuracy measured across all 100 novel classes of Caltech-UCSD Birds. 'H' denotes the High-Order Integration and 'Att' means Focus-area Location. '(ori)' means the original data in the paper and '(re)' represents the data we re-implement with ResNet as backbone feature extractor.

N -shot	1	2	5
Imprint(ori) [47]	44.75%	48.21%	52.95%
Imprint(ori) + Aug	44.60%	48.48%	52.78%
Imprint(re)	44.68%	52.19%	59.27%
ResNet + H	45.72%	52.64%	59.96%
ResNet + CNloss	45.06%	51.69%	58.73%
ResNet + CNloss + H	47.23%	54.38%	60.27%
ResNet + CNloss + H + Att	47.89%	54.83%	61.30%

TABLE II: Top-1 accuracy measured across base plus novel categories of Caltech-UCSD Birds.

E. mini DogsNet

Hilliard et al. [15] created a *miniDogsNet* which consists images of dog categories from the ImageNet to test the model's fine-grained ability. They selected 100 of those classes and use the 64/16/20 random classes split for training, validation, and testing. In our work, we further increase the difficulty by random selecting 10 of 64 classes to form our training set. That means only 10 classes are used for training the feature extractor and 20 novel classes should be distinguished. And we train the ResNet18 [5] from scratch.

We conduct 5-way experiments with both 1-shot and 5-shot trials. Table III shows that our model could achieve promising performance both on 1-shot and 5-shot tasks. To verify the effectiveness of our different modules, we use the ResNet18 and cosine classifier as the baseline. To our surprise, the baseline can also achieve nice performance. Relation Nets [6] uses the deep non-linear metric to capture the similarity between samples and is well performed even using 10 classes training data. For our method, we can see that CN_Loss and high-order integration can bring promising improvements. And the focus-area location mechanism is still beneficial to the task.

F. mini PPlankton

Currently, datasets for few-shot learning is usually resampled from the existing large-scale datasets. In fact, even for novel categories with only a few labeled samples, the external labeled images could be obtained by searching for free web-data. Nevertheless, for a real-world task in specific domain

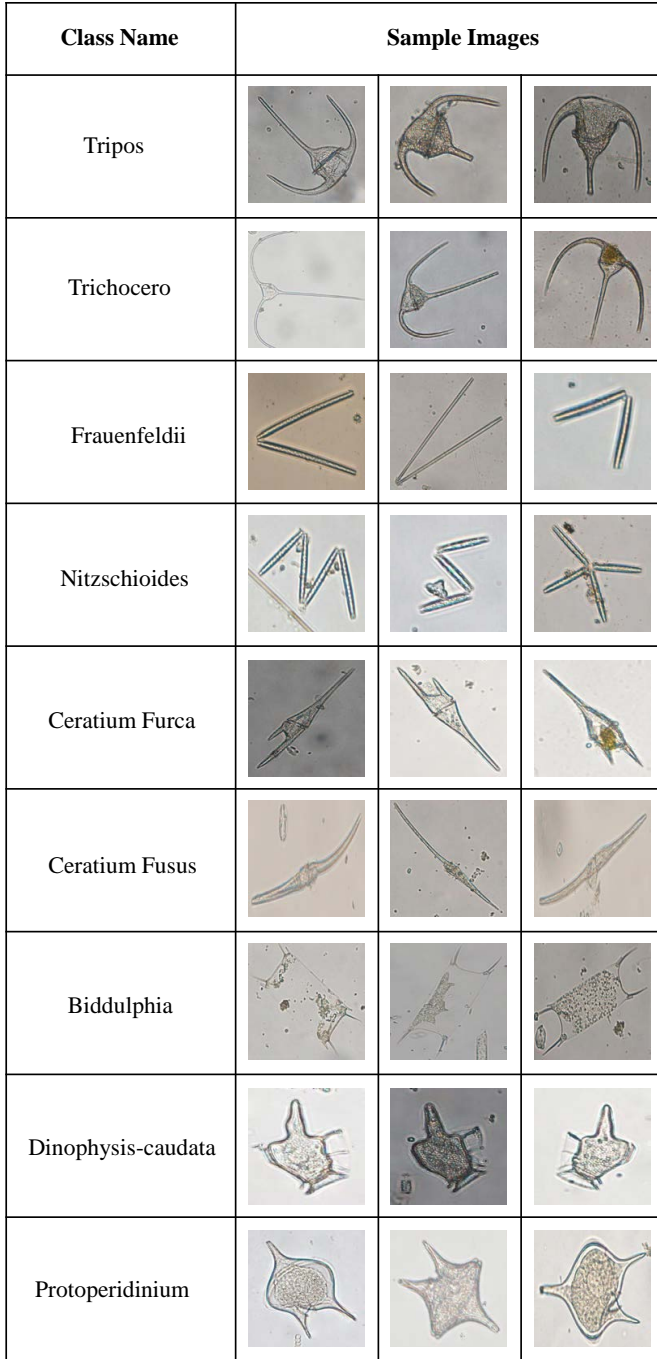


Fig. 9: Random samples of nine categories from our Phytoplankton dataset. The morphological differences among different categories are very small (such as the first two categories). It is a typical dataset for fine-grained challenge problem.

such as phytoplankton classification, it is infeasible to collect large-scale samples and it always requires experts to label the data. Meanwhile, it is also quite difficult to search for the relevant open-source web-data. Current monitoring systems (e.g. UVP5, ZooScan and FlowCAM [58], [59], [60]) yield large amounts of images every day. It requires many marine biologists to manual classify the sample images. Nevertheless, new and scarce categories are valuable for marine science. To

5way N -shot	Dist.	1	5
Matching Net [13]	Cosine	30.39%	37.97%
Prototypical Net [14]	Euclid.	31.37%	39.33%
Relation Net[16]	Deep metric	32.42%	38.53%
MAML [55]	-	26.66%	35.60%
Imprint [47]	Cosine	30.14%	38.31%
Resnet + H	Cosine	30.17%	38.77%
ResNet + CNloss	Cosine	31.25%	40.63%
ResNet + CNloss + H	Cosine	31.95%	41.40%
ResNet+CNloss+H+Att	Cosine	33.13%	42.53%

TABLE III: The top-1 accuracy on the test set of *miniDogsNet*, all accuracy results are averaged over 100 test episodes and each episode contains 100 query samples from 5 classes. All results are reported with 95% confidence intervals.

N -shot	Dist.	1	5
Prototypical Net	Euclid.	50.84%	66.67%
Matching Net	Cosine.	48.76%	60.78%
Relation Net	Deep-metric	46.79%	58.48%
MAML	-	46.0%	60.63%
Imprint	Cosine	57.72%	72.99%
ResNet + CNloss	Cosine	59.0%	74.84%
ResNet + CNloss + H	Cosine	56.29%	70.8%
ResNet + CNloss + Att	Cosine	60.03%	75.56%

TABLE IV: The top-1 accuracy on the test set of *miniPPlankton*, all accuracy results are averaged over 100 test episodes and each episode contains 100 query samples from 5 classes. All results are reported with 95% confidence intervals.

address this real-world problem, we construct a phytoplankton dataset *miniPPlankton* for machine learning with the help of marine biologists. It is a particular image dataset for few-shot fine-grained classification problem.

Some examples of the dataset are shown in Fig. 9. To construct the dataset, we collect seawater samples from the Bohai Sea, and we photograph phytoplankton images contained in the sampled seawater by optical microscopes. With the help of marine biologists³, we label each object with its confident category. The *miniPPlankton* includes 20 classes each of which contains about 70 samples. From Fig. 9, we can observe that our dataset face the challenge problem of fine-grained classification. For example, their shapes between different categories are similar, such as tripes and trichocero.

For this dataset, we conduct 5-way experiments with both 1-shot and 5-shot trials on the \mathcal{D}_{novel} and we use the ResNet18 with cosine-classifier as the baseline (the same as Imprint). We randomly selected 10 classes as the basic training classes, and the remaining classes as the novel classes to evaluate few-shot tasks. As shown in table IV, we can see that the proposed model with CN_loss outperforms the baselines by a significant margin, from 62.88% to 64.63% in the 5-shot trial.

³The Institute of Oceanology, Chinese Academy of Sciences

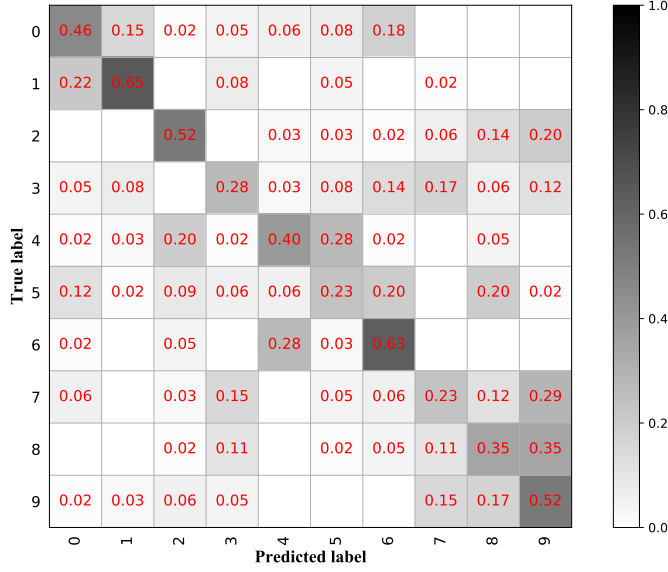


Fig. 10: The confusion matrix of the baseline (ResNet with cosine classifier, also equivalent to Imprint [47]).

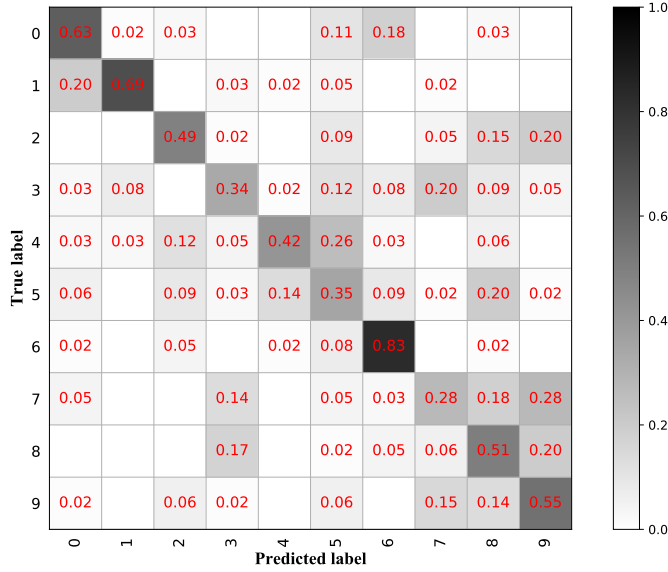


Fig. 11: The confusion matrix of our method.

However, to our surprise, the high-order module does not work for this dataset, and even leads to decline of test accuracy. The reason is that phytoplankton images are not "closed-shape" (target and background are separate) like normal images. For example, as shown in Fig. 9, the object of *Biddulphia* is interspersed with the background.

We further illustrate the improvement of classification performance for each category. Fig. 10 and Fig. 11 show the confusion matrices of the baseline and our method on \mathcal{D}_{novel} of *miniPPlankton*. We can see that our model greatly improves the accuracies of category 1 (pleurosigma-pelagicum) and category 6 (nitzschoides). At the same time, we reduce the possibility of misclassification of category 5 into category 6. However, it is still very challenge for some categories. Fig. 12

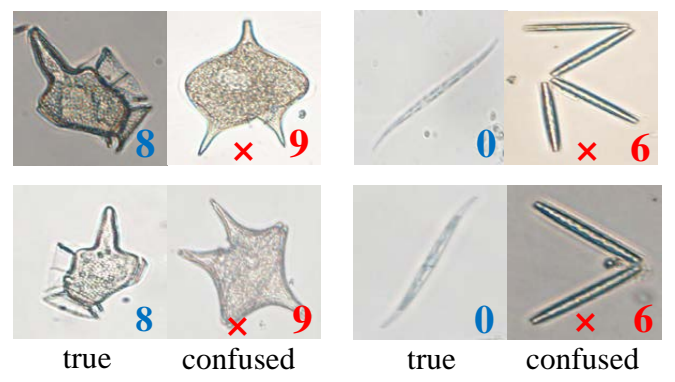


Fig. 12: The blue number in the lower right corner of the image represents the ground-truth category, and the red number represents the wrongly predicted category.

shows the most difficult category pairs. For instance, samples of category 8 are usually classify into category 9. It can be seen from Fig. 12 that the difference between these categories are very small. Such similarity even confuses marine biologists to distinguish them from each other.

V. CONCLUSION

In this paper, we focus on the challenge of the domain-specific few-shot fine-grained classification problem via exploring the attention features from one or a few labeled examples. The Feature Fusion Model and Center Neighbor Loss are our two contributions on mining features for such a challenge task. The fusion model utilizes the focus-area location and high-order integration to generate features from discriminative attention regions. As the fine-grained visual categories are quite similar to each other, we design Center Neighbor Loss to penalize the special samples which are difficult to approach class centers in each iteration. Extensive experiments are carried out to investigate the effects of these proposed modules. We achieved promising results on *miniDogsNet* dataset and Caltech-UCSD Birds. Furthermore, we build a typical fine-grained and few-shot learning dataset *miniPPlankton* from the real-world application in the area of marine ecological environment. We implement our model for the real-world phytoplankton recognition task. The experimental results show the superiority of the proposed model compared with state-of-the-art models on the *miniPPlankton* dataset. We believe that our method is a valuable complement to few-shot learning and the new *miniPPlankton* is attractive for this area.

ACKNOWLEDGMENT

This work is supported by the National Natural Science Foundation of China (No. U1706218 and No. 41576011).

REFERENCES

- [1] K. He, G. Gkioxari, P. Dollar, and R. Girshick, "Mask R-CNN," in *Proceedings of the IEEE International Conference on Computer Vision*, 2017, pp. 2980–2988.

- [2] H. Zhuang, K.-S. Low, and W.-Y. Yau, "Multichannel pulse-coupled-neural-network-based color image segmentation for object detection," *IEEE Transactions on Industrial Electronics*, vol. 59, no. 8, pp. 3299–3308, 2012.
- [3] Jia Deng, Wei Dong, R. Socher, Li-Jia Li, Kai Li, and Li Fei-Fei, "ImageNet: A large-scale hierarchical image database," in *2009 IEEE Conference on Computer Vision and Pattern Recognition*, 2009, pp. 248–255.
- [4] I. Dimitrovski, D. Koccev, I. Kitanovski, S. Loskovska, and S. Džeroski, "Improved medical image modality classification using a combination of visual and textual features," *Computerized Medical Imaging and Graphics*, 2015.
- [5] K. He, X. Zhang, S. Ren, and J. Sun, "Deep Residual Learning for Image Recognition," in *2016 IEEE Conference on Computer Vision and Pattern Recognition (CVPR)*, 2016.
- [6] G. Huang, Z. Liu, L. Van Der Maaten, and K. Q. Weinberger, "Densely connected convolutional networks," in *Proceedings - 30th IEEE Conference on Computer Vision and Pattern Recognition (CVPR)*, 2017, pp. 2261–2269.
- [7] B. M. Lake, R. Salakhutdinov, and J. B. Tenenbaum, "Human-level concept learning through probabilistic program induction," *Science*, vol. 350, pp. 1332–1338, 2015.
- [8] D. Swingley, "Fast mapping and slow mapping in children's word learning," *Language Learning and Development*, 2010.
- [9] J. Cui, B. Wei, C. Wang, Z. Yu, H. Zheng, B. Zheng, and H. Yang, "Texture and Shape Information Fusion of Convolutional Neural Network for Plankton Image Classification," *OCEANS*, 2018.
- [10] H. Ding, B. Wei, N. Tang, Z. Yu, N. Wang, H. Zheng, and B. Zheng, "Plankton Image Classification via Multi-class Imbalanced Learning," *OCEANS*, pp. 1–6, 2018.
- [11] H. Lee, M. Park, and J. Kim, "Plankton Classification on Imbalanced Large Scale Database via Convolutional Neural Networks with Transfer Learning," *IEEE International Conference on Image Processing (ICIP)*, pp. 3713–3717, 2016.
- [12] J. Liu, A. Du, C. Wang, Z. Yu, H. Zheng, B. Zheng, and H. Zhang, "Deep Pyramidal Residual Networks for Plankton Image Classification," *OCEANS*, 2018.
- [13] O. Vinyals, C. Blundell, T. Lillicrap, K. Kavukcuoglu, and D. Wierstra, "Matching Networks for One Shot Learning," *NIPS*, 2016.
- [14] J. Snell, K. Swersky, and R. S. Zemel, "Prototypical Networks for Few-shot Learning," *NIPS*, 2017.
- [15] N. Hilliard, L. Phillips, S. Howland, A. Yankov, C. D. Corley, and N. O. Hodas, "Few-Shot Learning with Metric-Agnostic Conditional Embeddings," *arXiv preprint arXiv:1802.04376*, 2018.
- [16] F. Sung, Y. Yang, L. Zhang, T. Xiang, P. H. S. Torr, and T. M. Hospedales, "Learning to Compare: Relation Network for Few-Shot Learning," *CVPR*, 2017.
- [17] S. Gidaris and N. Komodakis, "Dynamic Few-Shot Visual Learning without Forgetting," *CVPR*, 2018.
- [18] C. Wah, S. Branson, P. Welinder, P. Perona, and S. Belongie, "The Caltech-UCSD Birds-200-2011 Dataset," Tech. Rep., 2011.
- [19] J. Jiao, M. Zhao, J. Lin, and C. Ding, "Deep coupled dense convolutional network with complementary data for intelligent fault diagnosis," *IEEE Transactions on Industrial Electronics*, pp. 1–1, 2019.
- [20] X. Qi, B. Fang, L. Yi, J. Wang, Z. Jian, Y. Zheng, and G. Bao, "Automatic pearl classification machine based on multi-stream convolutional neural network," *IEEE Transactions on Industrial Electronics*, vol. PP, no. 99, pp. 1–1, 2017.
- [21] L. Zhang, Y. Gao, Y. Xia, Q. Dai, and X. Li, "A fine-grained image categorization system by cellet-encoded spatial pyramid modeling," *IEEE Transactions on Industrial Electronics*, vol. 62, no. 1, pp. 564–571, 2015.
- [22] Y. Taigman, M. Yang, M. Ranzato, and L. Wolf, "DeepFace: Closing the gap to human-level performance in face verification," in *Proceedings of the IEEE Computer Society Conference on Computer Vision and Pattern Recognition*, 2014.
- [23] Y. Sun, X. Wang, and X. Tang, "DeepID2: Deep Learning Face Representation by Joint Identification-Verification," *NIPS*, 2014.
- [24] X. Zhang, F. Zhou, Y. Lin, and S. Zhang, "Embedding Label Structures for Fine-Grained Feature Representation," *CVPR*, 2016.
- [25] J. Wang, Y. Song, T. Leung, C. Rosenberg, J. Wang, J. Philbin, B. Chen, and Y. Wu, "Learning fine-grained image similarity with deep ranking," in *CVPR*, 2014.
- [26] S. Chopra, R. Hadsell, and Y. LeCun, "Learning a similarity metric discriminatively, with application to face verification," in *IEEE Computer Society Conference on Computer Vision and Pattern Recognition (CVPR)*, 2005.
- [27] R. Salakhutdinov and G. Hinton, "Learning a nonlinear embedding by preserving class neighbourhood structure," *AISTATS*, 2007.
- [28] Y. Taigman, M. Yang, M. Ranzato, and L. Wolf, "Web-scale training for face identification," in *Proceedings of the IEEE Computer Society Conference on Computer Vision and Pattern Recognition*, 2015.
- [29] F. Schroff, D. Kalenichenko, and J. Philbin, "FaceNet: A unified embedding for face recognition and clustering," in *Proceedings of the IEEE Computer Society Conference on Computer Vision and Pattern Recognition*, 2015, pp. 815–823.
- [30] Y. Wen, K. Zhang, Z. Li, and Y. Qiao, "A discriminative feature learning approach for deep face recognition," in *Lecture Notes in Computer Science (including subseries Lecture Notes in Artificial Intelligence and Lecture Notes in Bioinformatics)*, vol. 9911 LNCS, 2016, pp. 499–515.
- [31] A. Vaswani, N. Shazeer, N. Parmar, J. Uszkoreit, L. Jones, A. N. Gomez, L. Kaiser, and I. Polosukhin, "Attention Is All You Need," *NIPS*, 2017.
- [32] I. Goodfellow and A. Odena, "Self-Attention Generative Adversarial Networks," *arXiv preprint arXiv:1805.08318*, 2018.
- [33] R. R. Selvaraju, M. Cogswell, A. Das, R. Vedantam, D. Parikh, and D. Batra, "Grad-CAM: Visual Explanations from Deep Networks via Gradient-Based Localization," in *Proceedings of the IEEE International Conference on Computer Vision*, 2017, pp. 618–626.
- [34] X. Zhang, Y. Wei, J. Feng, Y. Yang, and T. Huang, "Adversarial Complementary Learning for Weakly Supervised Object Localization," *CVPR*, 2018.
- [35] X. Wang, R. Girshick, A. Gupta, and K. He, "Non-local Neural Networks," *CVPR*, 2017.
- [36] B. Zhou, A. Khosla, A. Lapedriz, A. Oliva, and A. Torralba, "Learning Deep Features for Discriminative Localization," *CVPR*, 2016.
- [37] M. Lin, Q. Chen, and S. Yan, "Network In Network," *International Conference of Learning Representation*, 2014.
- [38] X. Wang, S. You, X. Li, and H. Ma, "Weakly-Supervised Semantic Segmentation by Iteratively Mining Common Object Features," *CVPR*, pp. 1354–1362, 2018.
- [39] O. Ronneberger, P. Fischer, and T. Brox, "U-net: Convolutional networks for biomedical image segmentation," in *Lecture Notes in Computer Science (including subseries Lecture Notes in Artificial Intelligence and Lecture Notes in Bioinformatics)*, 2015.
- [40] T. Y. Lin, P. Dollár, R. Girshick, K. He, B. Hariharan, and S. Belongie, "Feature pyramid networks for object detection," in *Proceedings - 30th IEEE Conference on Computer Vision and Pattern Recognition*, 2017.
- [41] S. Cai, W. Zuo, and L. Zhang, "Higher-Order Integration of Hierarchical Convolutional Activations for Fine-Grained Visual Categorization," *ICCV*, pp. 511–520, 2017.
- [42] R. J. Charlson, J. E. Lovelock, M. O. Andreae, and S. G. Warren, "Oceanic phytoplankton, atmospheric sulphur, cloud albedo and climate," *Nature*, 1987.
- [43] F. Zhao, F. Lin, and H. S. Seah, "School of Computer Engineering, Nanyang Technological University, Singapore 639798," *2009 16th IEEE International Conference on Image Processing (ICIP)*, pp. 2081–2084, 2009.
- [44] T. Luo, K. Kramer, D. B. Goldgof, S. Member, L. O. Hall, S. Samson, A. Remsen, and T. Hopkins, "Recognizing Plankton Images From the Shadow Image Particle Profiling Evaluation Recorder," *IEEE Transactions on Systems, Man, and Cybernetics, Part B (Cybernetics)*, vol. 34, no. 4, pp. 1753–1762, 2004.
- [45] E. C. Orenstein, O. Beijbom, E. E. Peacock, and H. M. Sosik, "WHOI-Plankton- A Large Scale Fine Grained Visual Recognition Benchmark Dataset for Plankton Classification," *CoRR*, 2015.
- [46] R. K. Simon-Martin Schröder, Rainer Kiko, Jean-Olivier Irissou, "Low-Shot Learning of Plankton Categories," *GCPR*, 2019.
- [47] H. Qi, M. Brown, and D. G. Lowe, "Low-Shot Learning with Imprinted Weights," *CVPR*, 2018.
- [48] Q. Wang, P. Li, and L. Zhang, "G2DeNet: Global Gaussian distribution embedding network and its application to visual recognition," in *Proceedings - 30th IEEE Conference on Computer Vision and Pattern Recognition, CVPR*, 2017.
- [49] N. Pham and R. Pagh, "Fast and scalable polynomial kernels via explicit feature maps," *Proceedings of the 19th ACM SIGKDD*, 2013.
- [50] H. Wang, Q. Wang, M. Gao, P. Li, and W. Zuo, "Multi-scale Location-Aware Kernel Representation for Object Detection," *CVPR*, pp. 1248–1257, 2018.
- [51] J. Fu, H. Zheng, and T. Mei, "Look closer to see better: Recurrent attention convolutional neural network for fine-grained image recognition," *CVPR*, pp. 4476–4484, 2017.
- [52] Y. Li, J. Zhang, J. Zhang, and K. Huang, "Discriminative Learning of Latent Features for Zero-Shot Recognition," *CVPR*, pp. 7463–7471, 2018.

- [53] Z. Chen, Y. Fu, Y. Zhang, Y.-G. Jiang, X. Xue, and L. Sigal, "Multi-level Semantic Feature Augmentation for One-shot Learning," *IEEE Transactions on Image Processing*, 2018.
- [54] G. Koch, R. Zemel, and R. Salakhutdinov, "Siamese Neural Networks for One-shot Image Recognition," *International Conference on Machine Learning*, 2015.
- [55] C. Finn, P. Abbeel, and S. Levine, "Model-Agnostic Meta-Learning for Fast Adaptation of Deep Networks," *International Conference on Machine Learning(ICML)*, 2017.
- [56] V. Garcia and J. Bruna, "Few-Shot Learning with Graph Neural Networks," *International Conference on Learning Representations(ICLR)*, 2017.
- [57] A. Calefati, M. K. Janjua, S. Nawaz, and I. Gallo, "Git Loss for Deep Face Recognition," *BMVC*, pp. 1–12, 2018.
- [58] R. K. Cowen and C. M. Guigand, "In situ ichthyoplankton imaging system (ISIIS): System design and preliminary results," *Limnology and Oceanography: Methods*, 2008.
- [59] G. Gorsky, M. D. Ohman, M. Picheral, S. Gasparini, L. Stemann, J. B. Romagnan, A. Cawood, S. Pesant, C. García-Comas, and F. Prejger, "Digital zooplankton image analysis using the ZooScan integrated system," 2010.
- [60] H. Jakobsen and J. Carstensen, "FlowCAM: Sizing cells and understanding the impact of size distributions on biovolume of planktonic community structure," *Aquatic Microbial Ecology*, 2011.